Brain Research 1846 (2025) 149229

Contents lists available at ScienceDirect

Brain Research

journal homepage: www.elsevier.com/locate/brainres

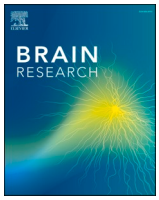

Registered Report Stage II

Associations between differential connectivity patterns of executive control networks and APOE ε4 in the Alzheimer continuum

Ruichen Han [a], Xue Zhang [b], Ya Chen [c], Xinle Hou [b], Feng Bai [b,d,e,*], for Alzheimer's Disease Neuroimaging Initiative[1]

[a] Department of Neurology, Nanjing Drum Tower Hospital Clinical College of Jiangsu University, Nanjing 210008, China
[b] Department of Neurology, Nanjing Drum Tower Hospital, Affiliated Hospital of Medical School, Nanjing University, Nanjing 210008, China
[c] Department of Neurology, Nanjing Drum Tower Hospital Clinical College of Traditional Chinese and Western Medicine, Nanjing University of Chinese Medicine, Nanjing 210008, China
[d] Geriatric Medicine Center, Taikang Xianlin Drum Tower Hospital, Affiliated Hospital of Medical School, Nanjing University, Nanjing 210008, China
[e] Institute of Geriatric Medicine, Medical School of Nanjing University, Nanjing 210008, China

ARTICLE INFO

Keywords:
Alzheimer
APOE
Executive control network
Resting-state fMRI

ABSTRACT

The APOE ε4 allele and age are risk factors for Alzheimer's disease (AD) and contribute to decreased executive function. However, the influence of APOE ε4 on the executive control network (ECN) in the AD continuum is still unclear. This study included 269 participants aged between 50 and 95 years old, based on ADNI data, including 104 cognitively normal (CN) individuals, 72 individuals with early mild cognitive impairment (EMCI), 55 individuals with late mild cognitive impairment (LMCI), and 38 AD patients. Within each disease group, participants were subdivided into APOE ε4 carriers and non-carriers. We explored brain regions within the ECN affected by the interactions between genes and disease states by resting-state functional magnetic resonance imaging (fMRI) and voxel-based two-way analysis of variance (ANOVA). Subsequently, functional connectivity (FC) between seeds and peak clusters were extracted and correlated with the cognitive performance. We found that the damages of carrying APOE ε4 in ECNs mainly distributed in the fronto-parietal and parietal-temporal systems. Functional network intergroup differences indicated increased intrafrontal and fronto-parietal connectivity at the early stage of AD and increased connectivity between the parietal lobe and related regions at late disease in these APOE ε4 carriers. Our conclusion is that the functional connectivity in the ECN exhibits different distinguishably patterns of impairment in the AD continuum under the influence of the APOE ε4 allele. Patients with different genotypes showed heterogeneity in functional network changes in the early stages of disease, which may be a potential biomarker for early AD.

1. Introduction

Alzheimer's disease (AD) is an irreversible neurodegenerative disease characterized by early symptoms of memory deficits followed by a progressive decline in multiple cognitive domains (Koutsodendris et al., 2022; Scheltens et al., 2021). Additional evidence suggested that executive dysfunction was also a core feature of preclinical AD (Mcguinness et al., 2010). Executive function refers to a set of high-level cognitive functions, including abstract reasoning, problem solving, and concept formation (Miyake et al., 2000; Hausman et al., 2022). Impairments in executive function can lead to abnormal activity in the human brain and can be detected by functional magnetic resonance imaging (fMRI) (Wang et al., 2011).

Some studies have found that the executive control network (ECN) is a broad brain region responsible for executive function and plays a crucial character in various attention-demanding cognitive tasks. The ECN is mainly anchored in the anterior cingulate cortex (ACC), dorsolateral prefrontal cortex (DLPFC), inferior parietal cortex (IPC), and left frontal insula, with extensive connections to other regions (Vincent et al., 2008; Yeo et al., 2011). The prefrontal cortex (PFC) has rich and complex fiber connections with other cerebral cortical and subcortical structures, and plays a pivotal role in higher cognitive functions. The

* Corresponding author.
E-mail address: baifeng@njglyy.com (F. Bai).

[1] Data used in preparation of this article were obtained from the Alzheimer's Disease Neuroimaging Initiative (ADNI) database (adni.loni.usc.edu).

https://doi.org/10.1016/j.brainres.2024.149229
Received 19 April 2024; Received in revised form 16 August 2024; Accepted 5 September 2024
Available online 8 September 2024

parietal cortex integrates various sensory inputs from the external environment with language. The frontal and parietal lobes not only exhibit extensive fiber connections but also show close functional correlations, essential for maintaining normal executive control functions. Pardo et al. (2007) demonstrated that altered function of the ACC, IPC and medial prefrontal cortex (i.e., low metabolism and reduced activation) was associated with poorer executive function performance, while the IPC was associated with the guidance of spatial attention (Pardo et al., 2007). Interestingly, cognitively unimpaired older adults exhibit hyperfunctional connectivity in the ECN with aging because older adults may invoke additional activities in brain regions. These enhanced activities play a crucial role in maintaining normal cognitive function (Grady et al., 2002). The same phenomenon could be observed in patients with MCI. Compared with that in controls, the connectivity of the frontoparietal network in the temporal and frontal regions in AD patients was significantly lower (Benson et al., 2018; Agosta et al., 2012). An accelerated decline in executive function occurs 2–3 years before clinical AD diagnosis, and changes in executive network connectivity may occur even earlier. Exploring the functional connectivity (FC) changes in the ECN in AD spectrum patients can help in the early identification and diagnosis of AD.

The apolipoprotein E (APOE) ε4 allele increases the risk of AD by promoting the aggregation of extracellular amyloid (aβ) plaques (Wang et al., 2015; Mcdade et al., 2021; Raulin et al., 2022). APOE ε4 is associated with memory deterioration and accelerated cognitive decline (Mishra et al., 2018; Caselli et al., 2009). APOE risk genes also play a role in regulating intrinsic functional networks in cognitively healthy individuals. Healthy elderly people with APOE ε4 mutation carriers exhibit a complex pattern of greater default mode network (DMN) connectivity in early adulthood (Filippini et al., 2009) than non-carriers and reduced functional connectivity later in life (Brown et al., 2011). Similarly, Ye et al. (2017) reported that ε4 carriers had a longitudinal increase in FC in the left hippocampus (HIP.L) and the right frontal area in normal subjects but a decrease in aMCI patients. With cognitive decline, APOE ε4 carriers exhibit greater functional inactivation of brain regions. However, the effect of the APOEε4 mutation on ECN is well defined, and longitudinal changes in AD progression have not been described.

Therefore, we wanted to explore how the APOE ε4 allele affects brain ECN connectivity and executive function during the development of AD-spectrum. We proposed the following hypotheses: (i) cognitively normal individuals carrying the APOE ε4 allele experience an earlier decline in executive function and exhibit compensatory changes in ECN functional connectivity; (ii) with disease progression and cognitive decline, when compensatory functional connectivity changes are insufficient to maintain cognitive function, the patterns of ECN functional connectivity in APOE ε4 allele carriers and non-carriers gradually become different.

2. Materials and methods

2.1. Subjects

The participants included in this study were sletcted from the ADNI database. The ADNI is a multicenter collaborative open source database aimed at identifying biomarkers for diagnosing and predicting AD. More details and thorough introduction can be found in ADNI official website (https://adni.loni.usc.edu). This study included 269 participants aged between 50 and 95 years, including 104 in the cognitively normal (CN) group, 72 in the early mild cognitive impairment (EMCI) group, 55 in the late mild cognitive impairment (LMCI) group, and 38 in the AD group. In each group, individuals are classified as carriers or non-carriers based on whether they carry the APOE ε4 allele. The inclusion and diagnostic criteria met the requirements of the ADNI manual. We screened all subjects in the ADNI database, and patients had to have available MMSE, MoCA, structural MRI and resting-state fMRI to be included in the study. In addition, any subject without a clear APOE ε4 carrier status would be excluded from the analysis. After quality screening and data preprocessing, the subjects with large head movement and poor registration were excluded. We extracted the following variables for analysis: sex, age, years of education, Mini-Mental State Examination (MMSE) score, clinical dementia rating sum of boxes (CDRSB), Montreal Cognitive Assessment (MoCA), Logical Memory-Delayed Recall (LDELTOTAL), Alzheimer's Disease Assessment-Cognition 11 items (ADAS11), ADAS-Cognition 13 items (ADAS13), score from Task 4 (Word Recognition) of the Alzheimer's Disease Assessment Scale (ADASQ4), scores for Trail Making Test Parts B (TRABSCOR), florbapir 18F (AV45, a highly sensitive and specific positron emission tomography (PET) molecular biomarker) and total score of the Functional Activities Questionnaire (FAQ). The Trail Making Test is the most popular neuropsychological task used for the clinical evaluation of executive function. In Part B of this test, participants were asked to connect the numbers and letters in 25 circles in both numeric and alphabetical order, using alternating numbers and letter, and a letter needed to be inserted between the two numbers in order. It is sensitive to executive dysfunction and has shown consistent results across multiple clinical populations. The RAVLT is a widely used, reliable, and effective auditory speech learning and memory assessment tool (Brugnolo et al., 2014).

2.2. MRI acquisition

All patients and normal subjects enrolled in this study underwent 3.0-Tesla MR imaging. As these participants underwent examinations at different sites, the machines used included Philips Medical Systems Intera, GE MEDICAL SYSTEM, and Siemens. T2-weighted resting-state fMRI images were obtained by planar echo imaging sequence with the following parameters: repetition time = 3,000 ms; echo time = 30 ms; number of slices = 48; and slice thickness = 3.3 mm; spatial resolution = $3 \times 3 \times 3$ mm^3. The time point, flipping angle, and matrix may differ due to the scanning machine used, but these factors do not affect the analysis results. Anatomical features were acquired from T1-weighted sequences. The specific parameters can be found in the appendix. All magnetic resonance images were evaluated by the ADNI MRI quality control center. For detailed information on the ADNI MRI data acquisition protocol, please refer to the official website of the ADNI (https://adni.loni.usc.edu/methods/mri-tool/mri-analysis/).

2.3. MRI data preprocessing

The rs-fMRI images were preprocessed by Toolkit for rs-fMRI Data Analysis (https://restfmri.net) and SPM12 software package (https://www.fil.ion.ucl.ac.uk/spm/) in MATLAB 2022a. Preprocessing included the following steps: (1) discarding the first 10 time points to ensure stable-state magnetization and to allowing subjects to acclimate to the scanning noise; (2) performing slices correction, aiming at correcting the differences in image acquisition time between slices; (3) performing head movement correction; (4) registering structural and functional images onto the Montreal Neurological Institute (MNI) space for standardization by deformation field generation; (5) resampling (voxel size = 3 mm × 3 mm × 3 mm); (6) using an isotropic Gaussian kernel with a full width half maximum of 6 mm for spatial smoothing; (7) removing linear trends, which are caused by the accumulation of time causing the scanner to heat up or participants to adapt; (8) regressing the effects of head movement in 6 directions from fMRI data, cerebrospinal fluid and white matter signal noise; and (9) band-pass filtered, retain specific frequencies (0.01–0.08 Hz) to regressing out low-frequency noise caused by physiological activities, such as breathing and cardiac activity. Among all participants, 58 were excluded due to significant registration errors, with an average frame displacement greater than 3.0 mm or a maximum rotation exceeding 3.0 degrees.

2.4. Definition of the ECN masks and FC analysis

Core regions of the ECN (or "central executive") network are in the DLPFC and inferior parietal lobe (IPL). These two regions are significantly activated during cognitively demanding tasks and are the core nodes of the ECN (Cai et al., 2017). There are a large number of methods for analysing functional connectivity, including voxel-based or seed-based Pearson's correlation analysis, amplitude of low frequency fluctuation, independent component analysis, principal component analysis, graph theory measurement, dynamic functional connectivity (Zhao et al., 2019; Wee et al., 2014; Esposito and Goebel, 2011). Pearson correlation is widely used to extract functional networks. The network obtained through ROI based methods is highly consistent with that obtained through cognitive tasks (He et al., 2014; Biswal et al., 1995; Song et al., 2016). The definitions of the four ROIs in the ECN are based on previous task-state fMRI studies (Duan et al., 2012); including the left DLPFC (MNI coordinates: −48,34,34), the right DLPFC (MNI coordinates: 48,40,30), the left IPL (MNI coordinates: −36, −44,46) and the right IPL (MNI coordinates: 42, −42,48).

The average blood oxygen level dependent (BOLD) signal time series were extracted from 6 mm radius spheres centered at the peak coordinates of each ROI, and the pearson correlation coefficients were computed between these average time series and the time series of all voxels in the whole brain, resulting in the whole-brain functional connectivity maps. To adjust the correlation coefficients distribution, Fisher Z-transform was applied to normalize it. We subsequently conducted connectivity analysis and selected the familywise error (FWE) method with a threshold of $p < 0.05$ to correct for multiple comparisons to obtain ECN network maps. The identified brain regions were positively correlated with the ECN ROI, and the ECN network maps of the eight subgroups were combined to obtain the ECN spatial distribution and used as a mask.

2.5. Statistical analysis

For demographic information, the normality of data distribution was examined using P-P plots. $\chi 2$ two-tailed test was employed for gender variable. One-way ANOVA was used for age, years of education, RAVLT_learning, and LDELTOTAL that met homogeneity of variance. Welch's test was utilized for demographic variables that did not meet the criteria of normal distribution.

To determine the brain regions affected by the interaction between all subgroups at the voxel-level, a two-way ANCOVA was performed for APOE status (i.e., carrying and not carrying alleles) and disease status (i.e., CN, EMCI, LMCI, AD), with age, sex, total intracranial volume, and education level added as covariates. The thresholds were set at a corrected $p < 0.05$, determined by Monte Carlo simulation for multiple comparisons (AlphaSim-corrected voxel-wise $p < 0.01$, FWHM=6 mm, cluster size = 38 mm^3). Then, *post-hoc* analysis were performed to determine the details of the changes in the FC patterns of interaction brain regions between subgroups. Finally, partial correlation analysis was used to investigate the relationship between cognitive scores and functional connectivity in different disease states (CN, EMCI, LMCI and AD), controlling variables such as gender, years of education and age. All analyses of demographic characteristics and behavioral correlations were performed with the use of SPSS Statistics 27 (https://www.ibm.com/cn-zh).

3. Experimental design

The experimental procedure for this study is detailed in Fig. 1. The subjects included in this study were enrolled in the ADNI database between September 2005 and March 2023. Some of the subjects because of a lack of demographic data (APOE gene type is not clear) and neuropsychological testing data were excluded from analysis. All subjects included in the analysis underwent structural magnetic resonance and resting-state functional magnetic resonance scans, and data preprocessing was performed to ensure that the data quality was within acceptable limits. A total of 269 eligible subjects were included and divided into four groups according to the following criteria: (1) CN group: MMSE score between 24 and 30, CDR=0, no complaints of depression, cognitive decline and psychiatric symptoms, age roughly matched with MCI and AD; (2) EMCI group: MMSE score between 24 and 30, complaints of memory decline and objective memory loss, CDR score 0.5 after adjustment for education level, and no impairment in daily life; (3) LMCI group: MMSE score in the 24 to 30 points, a multiple

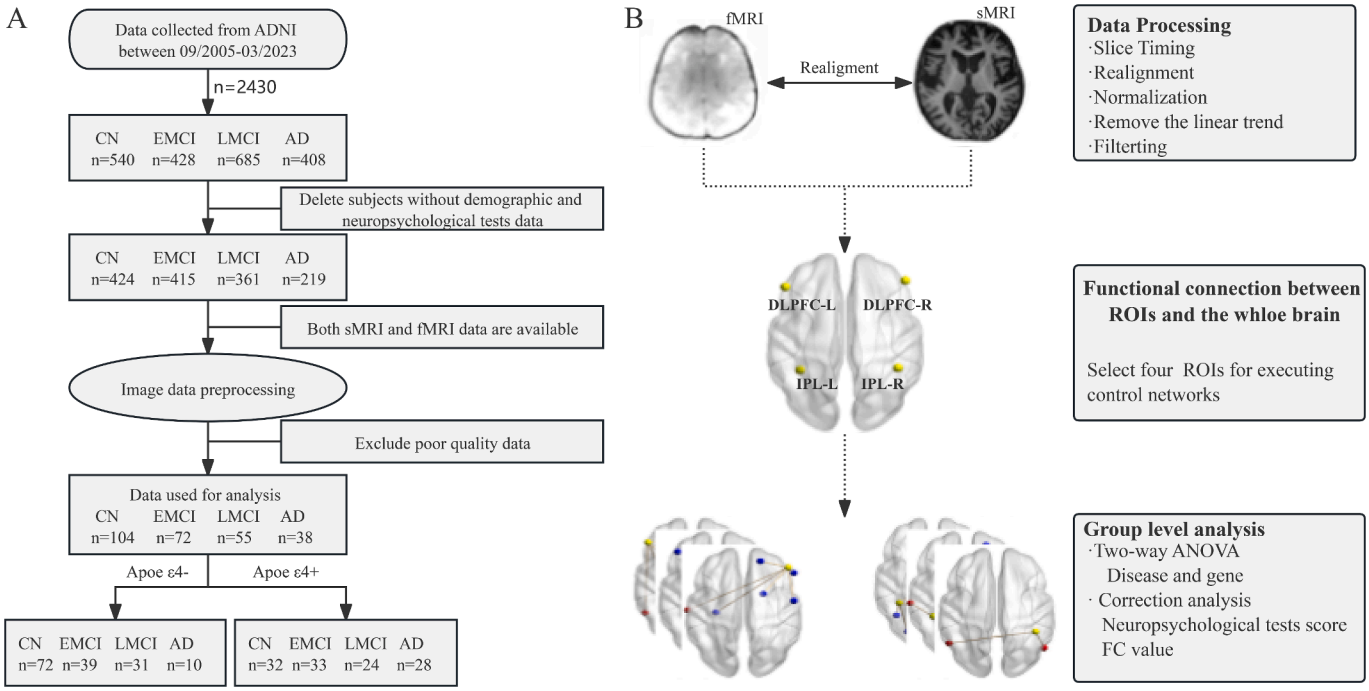

Fig. 1. A summary of the analysis framework in this study.

cognitive domain are obvious function to drop, and affect daily life function; (4) the AD group MMSE score between 20 and 26 points, CDR is 0.5 or 1.0, and in accordance with internationally recognized AD diagnostic criteria.

Exclusion criteria: (1) use of cholinergic antidepressants, neuroleptic drugs, or prolonged use of narcotic analgesics, etc.; (2) history of severe psychiatric illness; (3) History of head trauma or stroke; (4) other central nervous system diseases that may cause cognitive decline; (5) severe mental health conditions such as schizophrenia, anxiety, and depression; (6) severe systemic diseases such as heart failure and renal dysfunction; (7) MRI intolerance or inability to complete neuropsychological testing. All subjects included in the ADNI database met these exclusion criteria.

The fMRI data underwent a series of preprocessing steps including temporal slice timing correction and co-registration with structural images. Subsequently, seed points were selected to construct the ECN and compute voxel-wise whole-brain functional connectivity. Finally, between-group two-way ANOVA and post-hoc tests were conducted.

4. Results

4.1. Demographic and neuropsychological performance

The results were presented in Table 1, included a total of 104 CN (32

Table 1
Demographic and neuropsychological data.

Items	CN		EMCI		LMCI		AD		F/χ^2	P
	Apoe ε4-	Apoe ε4+	Apoe ε4-	Apoe ε4+	Apoe ε4-	Apoe ε4+	Apoe ε4-	Apoe ε4+		
	(n = 72)	(n = 32)	(n = 39)	(n = 33)	(n = 31)	(n = 24)	(n = 10)	(n = 28)		
DEMOGRAPHICS										
Age (years)	75.21 ± 8.12	75.03 ± 7.73	74 ± 7.73	72.21 ± 6.44	72.65 ± 9.2	73.79 ± 7.7	74.08 ± 7.29	72.26 ± 7.51	1.305	0.248
Gender(M/F)	30/45	14/18	17/24	23/16	21/11	13/10	4/8	17/17	12.112	0.097
Education (years)	16.57 ± 2.45	16.28 ± 2.36	16.29 ± 2.73	15.87 ± 2.81	15.9 ± 2.29	16.46 ± 3.05	15.17 ± 2.59	15.29 ± 2.57	1.503	0.166
GENERAL COGNITION										
CDRSB	0.02 ± 0.1	0 ± 0	1.24 ± 1.07[a]	1.28 ± 1.11[a]	1.58 ± 1.11[a]	1.77 ± 1.11[a]	4.17 ± 2.52[ab]	4.59 ± 1.33[ab]	90.387	<0.001*
MMSE	29 ± 1.24	28.75 ± 1.37	28.54 ± 1.47	27.9 ± 1.83[a]	27.77 ± 1.8[a]	27.33 ± 2.18[a]	23.5 ± 2.28[ab]	22.5 ± 2.49[ab]	31.832	<0.001*
MOCA	26.53 ± 2.51	25.47 ± 2.82	24.12 ± 2.21	23.72 ± 2.98[a]	22.1 ± 3[a]	22.98 ± 3.45[a]	18.58 ± 3.4[ab]	15.78 ± 4.78[ab]	25.089	<0.001*
SCORES OF EACH COGNITIVE DOMAIN										
Cognition										
ADAS11	5.02 ± 2.34	5.35 ± 3.48	7.98 ± 3.12[a]	8.6 ± 3.75[a]	10.48 ± 4.95[a]	10.24 ± 4.22[a]	16.83 ± 5.6[ab]	22.8 ± 7.44[ab]	32.384	<0.001*
ADAS13	7.79 ± 3.84	8.42 ± 5.52	12.26 ± 4.51[a]	13.92 ± 5.97[a]	16.39 ± 7.38[a]	16.49 ± 6.71[a]	26.67 ± 7.59[ab]	33.98 ± 8.64[ab]	42.186	<0.001*
Delayed Recall										
ADASQ4	2.43 ± 1.8	2.47 ± 1.97	3.8 ± 1.84[a]	4.6 ± 2.2[a]	5.06 ± 2.73[a]	5.63 ± 2.65[a]	7.75 ± 2.05[ab]	8.97 ± 1.17[ab]	69.269	<0.001*
LDELTOTAL	14.15 ± 3.37	13.84 ± 4.06	9.37 ± 2.74[a]	9.35 ± 3.44[a]	5 ± 2.57[a]	4.21 ± 2.47[a]	1.75 ± 2.63[ab]	1.44 ± 1.93[ab]	84.823	<0.001*
Aβ level										
AV45	1.11 ± 0.14	1.21 ± 0.23	1.15 ± 0.22[a]	1.35 ± 0.19[a]	1.24 ± 0.24[a]	1.26 ± 0.2[a]	1.36 ± 0.26[a]	1.5 ± 0.15[ab]	20.621	<0.001*
Social Function										
FAQ	0.08 ± 0.32	0.14 ± 1.1	2.62 ± 3.65[a]	2.27 ± 3.73[a]	3.68 ± 3.43[a]	5.13 ± 5.76[a]	12.25 ± 7.82[ab]	15.62 ± 6.66[ab]	30.001	<0.001*
Episodic Memory										
RAVLT_forgetting	3.28 ± 2.84	3.88 ± 2.43	4.86 ± 1.93[a]	4.69 ± 2.31[a]	4.1 ± 2.21	5.5 ± 1.91[a]	5.25 ± 2.38[a]	4.24 ± 1.39[a]	3.695	<0.001*
RAVLT_immediate	48.37 ± 10.78	44.66 ± 10.61	37.45 ± 9.11[a]	36.18 ± 10.11[a]	32.45 ± 8.65[a]	33.38 ± 7.63[a]	26.75 ± 7.53[ab]	21.65 ± 6.13[ab]	39.201	<0.001*
RAVLT_learning	6.11 ± 2.58	6.09 ± 2.31	5.61 ± 2.62	4.21 ± 2.35[a]	3.61 ± 2.23[a]	3.25 ± 2.09[a]	2.17 ± 2.12[a]	1.38 ± 1.69[ab]	17.691	<0.001*
RAVLT_perc_forgetting	30.45 ± 28.28	35.39 ± 24.15	55.14 ± 29.06[a]	57.04 ± 30.66[a]	53.79 ± 30[a]	73.9 ± 27[a]	85.6 ± 27.38[ab]	94.6 ± 15.8[ab]	31.012	<0.001*
Executive Functions										
TRABSCOR	73.96 ± 35.85	93.28 ± 59.65	101.87 ± 58.82[a]	101.33 ± 56.23[a]	120.75 ± 63.7[a]	113.04 ± 74.24[a]	187.06 ± 92.53[ab]	216.55 ± 72.89[ab]	18.392	<0.001*

−Values are presented as the mean ± standard deviation (SD). The p-value was obtained by one-way ANOVA. * Indicates a statistical difference between groups, $p < 0.001$.

CN, normal aging / cognitively normal; EMCI, early mild cognitive impairment; LMCI, late mild cognitive impairment; AD, Alzheimer's disease; CDRSB, clinical dementia rating scale sum of boxes; MMSE, mini mental state examination; MoCA, montreal cognitive assessment; ADAS11, Alzheimer's Disease Assessment Scale-Cognition 11 items; ADAS13, ADAS-Cognition 13 items; ADASQ4, Score from Task 4 (Word Recognition) of the Alzheimer's Disease Assessment Scale; AV45, Reference region − florbetapir mean of whole cerebellum; FAQ, Functional Activities Questionnaire; LDELTOTAL, Logical Memory − Delayed Recall; RAVLT, the Rey Auditory Verbal Learning Test; immediate, the sum of scores from 5 first trials (Trials 1 to 5); learning, the score of Trial 5 minus the score of Trial 1; forgetting, the score of Trial 5 minus score of the delayed recall; perc_forgetting, percent forgetting − RAVLT Forgetting divided by the score of Trial 5; TRABSCOR, the score of Trails B.

[a]$P < 0.05$, compared with CN;[b]$P < 0.05$, compared with MCI;

ε4 allele carriers and 72 non-carriers), 72 EMCI (33 ε4 allele carriers and 39 non-carriers), 55 LMCI (24 ε4 allele carriers and 31 non-carriers) and 38 AD (28 ε4 allele carriers and 10 non-carriers) subjects were included. The results revealed no significant differences between the 8 groups in terms of age, sex, or levels of education. *Post-hoc* analysis using LSD correction showed that cognitive ability test scores were greater in the AD subgroup than in the CN and MCI subgroups, as indicated by the CDRSB, RAVLT_perc_forgetting, TRABSCOR, ADAS11/13, ADASQ4 and FAQ scores (more details can be found in Table 1).

4.2. Disease × gene interaction ANOVA of ECN functional connectivity

Table 2 and Fig. 2 show the coordinates and spatial distribution of brain regions with significant differences between groups in the main and interactive effects of disease and risk gene. Two-way ANOVA was used to identify the difference in FC across groups within the ECN mask. The statistical threshold was set at a corrected $p < 0.05$ (AlphaSim-corrected).

(1) In the L-DLPFC network, the regions most affected by the disease were the insula (INS), prefrontal cortex, parietal cortex and temporal gyrus (i.e., left INS, right supraorbital gyrus, right superior frontal orbital part gyrus, and left inferior temporal gyrus). However, the regions affected by APOE ε4 gene were not significantly different. The region of the parietal lobe (the paracentral lobule (PCL)) is influenced by both genetic and disease factors.

(2) In the R-DLPFC network, brain regions associated with main disease effects were found in the frontal lobe (i.e., right dorsolateral superior frontal gyrus, MFG, and precental gyrus), temporal lobe (i.e., left middle temporal gyrus), and HIP.L. The brain regions related to the genes were mainly distributed in the right middle occipital gyrus (MOG). Notably, the roles of the bilateral MFG are different, with the left MFG being influenced mainly by genes and the right MFG being affected by disease.

(3) In the L-IPL network, a wide range of brain regions, including the right inferior frontal gyrus (opercular part), left angular gyrus (ANG), left precuneus (PCUN), right middle occipital gyrus, right inferior temporal gyrus and left posterior cingulate gyrus (PCG.L), were shown to be affected by the main effect of the disease. The regions affected by the main effect of the gene were mainly distributed in the frontal and temporal lobes, specifically the right rolandic operculum, bilateral superior temporal gyrus (STG), right inferior temporal gyrus, superior frontal gyrus and anterior cingulate gyrus. In particular, regions associated with gene × disease interactions were in the left middle temporal gyrus (MTG) and right superior frontal orbital gyrus.

(4) In the R-IPL network, the right PCUN, left amygdala and right calcarine fissure and surrounding cortex were significantly

Table 2
Disease × gene ANOVA of executive control network functional connectivity.

		Region(aal)	x(mm)	y(mm)	z(mm)	Cluster size(mm3)	Peak F-value
DLPFC-L	Main effect of disease	Insula_L (aal)	−36	3	6	85	8.2756
		Frontal_Sup_Orb_R (aal)	9	45	−24	68	7.8785
		Postcentral_R (aal)	12	−27	60	41	7.0926
		Temporal_Inf_L (aal)	−51	−57	−15	40	5.8586
	Main effect of gene	–	–	–	–	–	–
	Interaction: disease × gene	Paracentral_Lobule_L (aal)	−12	−27	72	65	5.5286
DLPFC-R	Main effect of disease	Frontal_Sup_R (aal)	18	48	48	104	7.0267
		Temporal_Mid_L (aal)	−60	−15	−18	91	7.1696
		Frontal_Sup_R (aal)	21	6	57	63	7.6219
		Hippocampus_L (aal)	−30	−18	−18	57	5.5800
		Precentral_R (aal)	54	−3	39	54	6.7040
		Frontal_Mid_R (aal)	54	33	21	40	5.6388
	Main effect of gene	Occipital_Mid_R (aal)	30	−93	18	100	16.3953
		Frontal_Mid_L (aal)	−42	39	21	68	12.5827
	Interaction: disease × gene	–	–	–	–	–	–
IPL-L	Main effect of disease	Frontal_Inf_Oper_R (aal)	45	15	15	417	7.0000
		Angular_L (aal)	−39	−60	42	102	6.6442
		Precuneus_L (aal)	−6	−45	42	83	5.0300
		Occipital_Mid_L (aal)	−27	−81	15	52	4.7358
		Temporal_Inf_R (aal)	51	−69	−15	50	8.0533
		Cingulum_Post_L (aal)	−6	−42	9	42	8.6909
	Main effect of gene	Temporal_Sup_R (aal)	66	−24	12	233	18.4974
		Frontal_Sup_R (aal)	21	48	24	98	17.4059
		Rolandic_Oper_R (aal)	60	9	3	74	13.8934
		Cingulum_Ant_L (aal)	0	36	27	64	10.9234
		Temporal_Sup_L (aal)	−60	−27	18	46	11.6943
		Temporal_Inf_R (aal)	66	−39	−21	41	14.0546
	Interaction: disease × gene	Temporal_Mid_L (aal)	−54	−51	3	59	5.8600
		Frontal_Sup_Orb_R (aal)	15	48	−12	53	8.0341
IPL-R	Main effect of disease	Precuneus_R (aal)	6	−54	48	105	5.0000
		Thalamus_L (aal)	3	−18	18	42	7.1885
		Calcarine_R (aal)	6	−54	9	40	6.2656
	Main effect of gene	Calcarine_L (aal)	3	−96	−9	455	16.5729
		Caudate_R (aal)	9	9	12	73	14.5317
	Interaction: disease × gene	Temporal_Mid_R (aal)	51	−63	3	193	7.6567
		Temporal_Mid_L (aal)	−51	−57	3	142	7.7500

MNI, Montreal Neurological Institute; L, left; R, right; DLPFC, dorsolateral prefrontal cortex; IPL, inferior parietal lobule. The thresholds were set at a corrected $P < 0.05$, determined by Monte Carlo simulation for multiple comparisons.

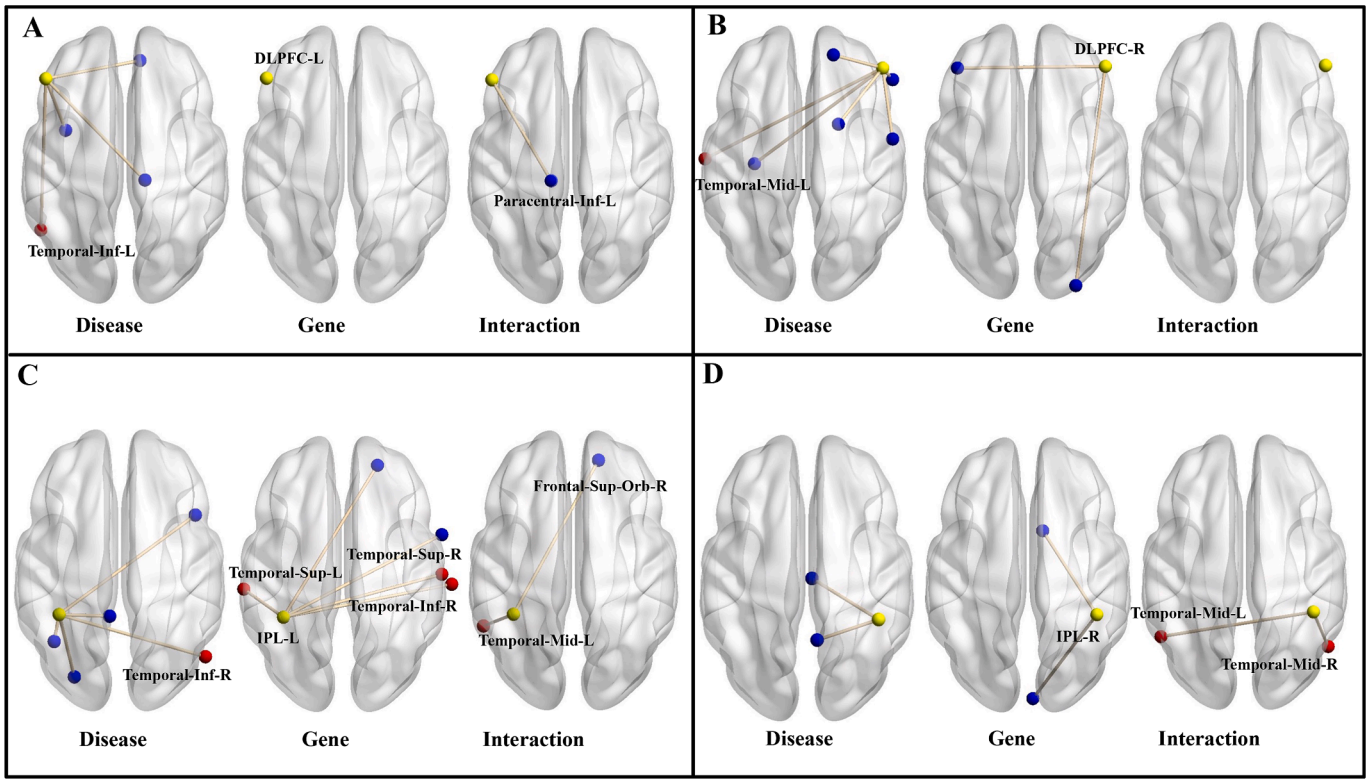

Fig. 2. Disease × gene ANOVA of the executive control network. The effects of disease, genetics and interactions on the L-DLPFC network (A), R-DLPFC network (B), L-IPL network (C) and R-IPL network (D). L, left; R, right; DLPFC, dorsolateral prefrontal cortex; IPL, inferior parietal lobule. The statistical threshold was set at $p < 0.05$, determined by Monte Carlo correction. Yellow: ROI; Blue: brain regions affected by the disease or genetic main effects; Red: brain regions (temporal lobe) affected by both disease and gene main effects. (For interpretation of the references to colour in this figure legend, the reader is referred to the web version of this article.)

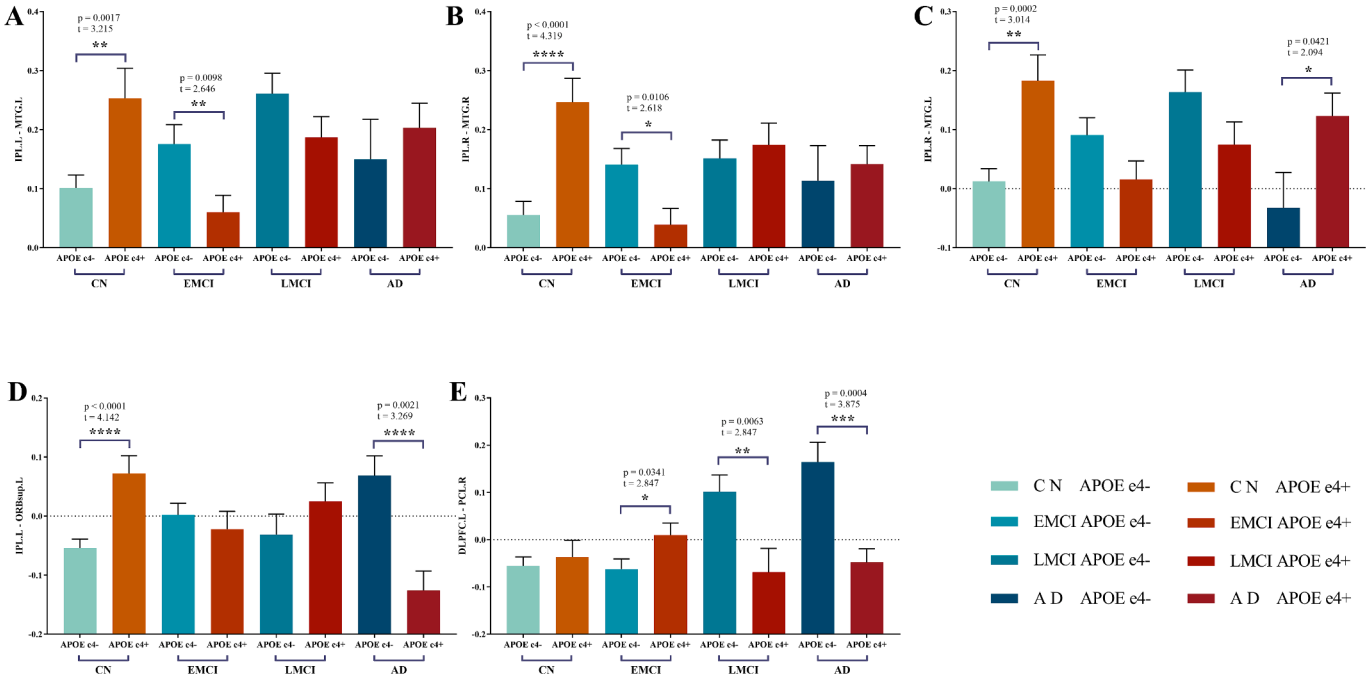

Fig. 3. Differences were observed between APOE ε4+ and APOE ε4- among the different groups, and APOE ε4+ was associated with the modification of the brain network. As the disease progresses, the parietal-temporal connections exhibit changes related to an inverted U-shaped curve (i.e., a trend of first decreasing and then increasing; A, B and C), while the pattern gradually becomes the opposite (i.e., U-shaped curve; D and E) in the parietal-frontal connection. L, left; R, right; IPL, inferior parietal lobule; DLPFC, dorsolateral prefrontal cortex; MTG, middle temporal gyrus; ORBsup, superior frontal gyrus, orbital region; PCL, paracentral lobule; CN, normal aging/cognitively normal; EMCI, early mild cognitive impairment; LMCI, late mild cognitive impairment; AD, Alzheimer's disease.

correlated with the main effect of the disease, while the left calcarine fissure and surrounding cortex and right caudate nucleus were correlated with the main effect of the gene. The interactions occurred mainly in the bilateral MTG.

4.3. Post-hoc analysis of ANOVA interaction

The *post-hoc* test reported significant differences in functional connectivity values between the ROIs and interaction regions between ε4 allele carriers and non-carriers. Fig. 3 illustrates these differences in rsFC between carriers and non-carriers within the same disease state. In the parietal-temporal network (i.e., IPL.L-MTG. L, IPL.R-MTG. R, and IPL.R-MTG. L), rsFC in non-carriers showed an initial increase followed by a decrease with disease progression, whereas in carriers, rsFC exhibited a decrease followed by an increase. In the frontal-parietal network (i.e., positive U-shaped curve, IPL.L-ORBsup.L (left superior frontal gyrus, orbital part) and DLPFC.L-PCL.R), carriers exhibited an overall decreasing trend in rsFC, while non-carriers showed an increasing trend. Across different stages of Alzheimer's disease, the APOE ε4 allele exerted varying effects on different functional connectivity loops within the ECN. In this study, we subtracted the functional connectivity values of non-carriers from those of carriers and performed Z-score standardization to display the difference between the two groups. As shown in Fig. 4, as the disease advanced, the difference of the parietal-temporal network showed changes related to an inverted U-shaped curve, while the pattern gradually became the opposite in the frontal-parietal network. The results indicated that as cognitive ability decreased, the difference in rsFC values between the parietal and temporal lobes of APOE ε4 carriers and no carriers tended to first decrease and then increase, while the FC between the DLPFC and the PCL showed the opposite trend.

4.4. Significance of ECN functional connectivity and cognitive scores

Fig. 5 presents the results of the correlation between cognitive scores and FC. Controlling for variables such as gender, years of education, and age, FC within the ECN was significantly correlated with cognitive scores. Given the potential influence of factors such as age, gender, and education level on both functional connectivity strength and cognitive scores, this study employed partial correlation analysis to mitigate these confounding factors. This approach aimed to more accurately assess the genuine associations between these variables.

4.4.1. L-DLPFC network

(1) Main effect of disease: Among the different brain regions affected by disease, we found a positive correlation between the episodic memory score (RAVLT_forgetting / perc_forgetting) of CN individuals and the FC of the left INS ($r = 0.224$, $p = 0.022$; $r = 0.228$, $p = 0.02$), while the delayed recall score (ADAQ4) was significantly positively correlated with the ORBsup.R ($r = 0.229$, $p = 0.019$). In the EMCI subgroup, there was a significant correlation between the FC of DLPFC.L to the right inferior temporal gyrus and Aβ horizontal ($r = 0.34$, $p = 0.002$). In the LMCI group, there was a significant correlation between ORBsup.R and RAVLT_immediate ($r = -0.324$, $p = 0.019$) and percent forgetting ($r = 0.276$, $p = 0.047$) in episodic memory. In the AD group, the ORBsup.R was significantly correlated with ADASQ4 scores ($r = 0.36$, $p = 0.018$), while the postcentral gyrus (PoCG) was associated with MoCA ($r = 0.308$, $p = 0.044$), MMSE ($r = 0.423$, $p = 0.005$), and RAVLT_immediate memory scores ($r = 0.349$, $p = 0.022$). (2) Main effect of gene: The brain regions affected by genetic main effects failed to pass correction for multiple comparisons. (3) Interaction of gene × disease: Among the brain regions with interactive effects, the FC values of DLPFC.R to PCL.L in LMCI patients were significantly correlated with ADAS11 and executive function (TRABSCOR), while AD patients were associated with

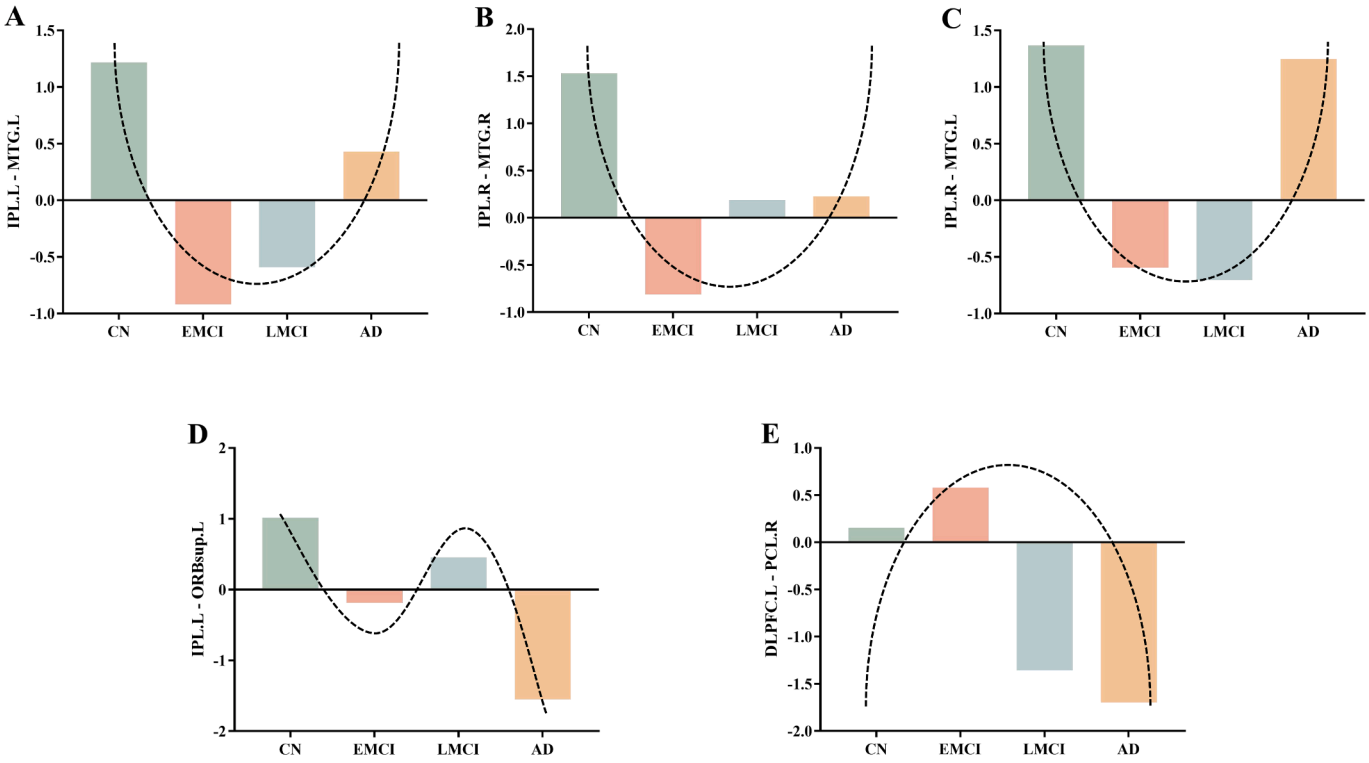

Fig. 4. Differences were observed between APOE ε4+ and APOE ε4- among the different groups, and APOE ε4+ was associated with the modification of the brain network. As the disease progresses, the parietal-temporal connections exhibit changes related to an inverted U-shaped curve (i.e., a trend of first decreasing and then increasing; A, B and C), while the pattern gradually becomes the opposite (i.e., U-shaped curve; D and E) in the parietal-frontal connection. L, left; R, right; IPL, inferior parietal lobule; DLPFC, dorsolateral prefrontal cortex; MTG, middle temporal gyrus; ORBsup, superior frontal gyrus, orbital region; PCL, paracentral lobule; CN, normal aging/cognitively normal; EMCI, early mild cognitive impairment; LMCI, late mild cognitive impairment; AD, Alzheimer's disease.

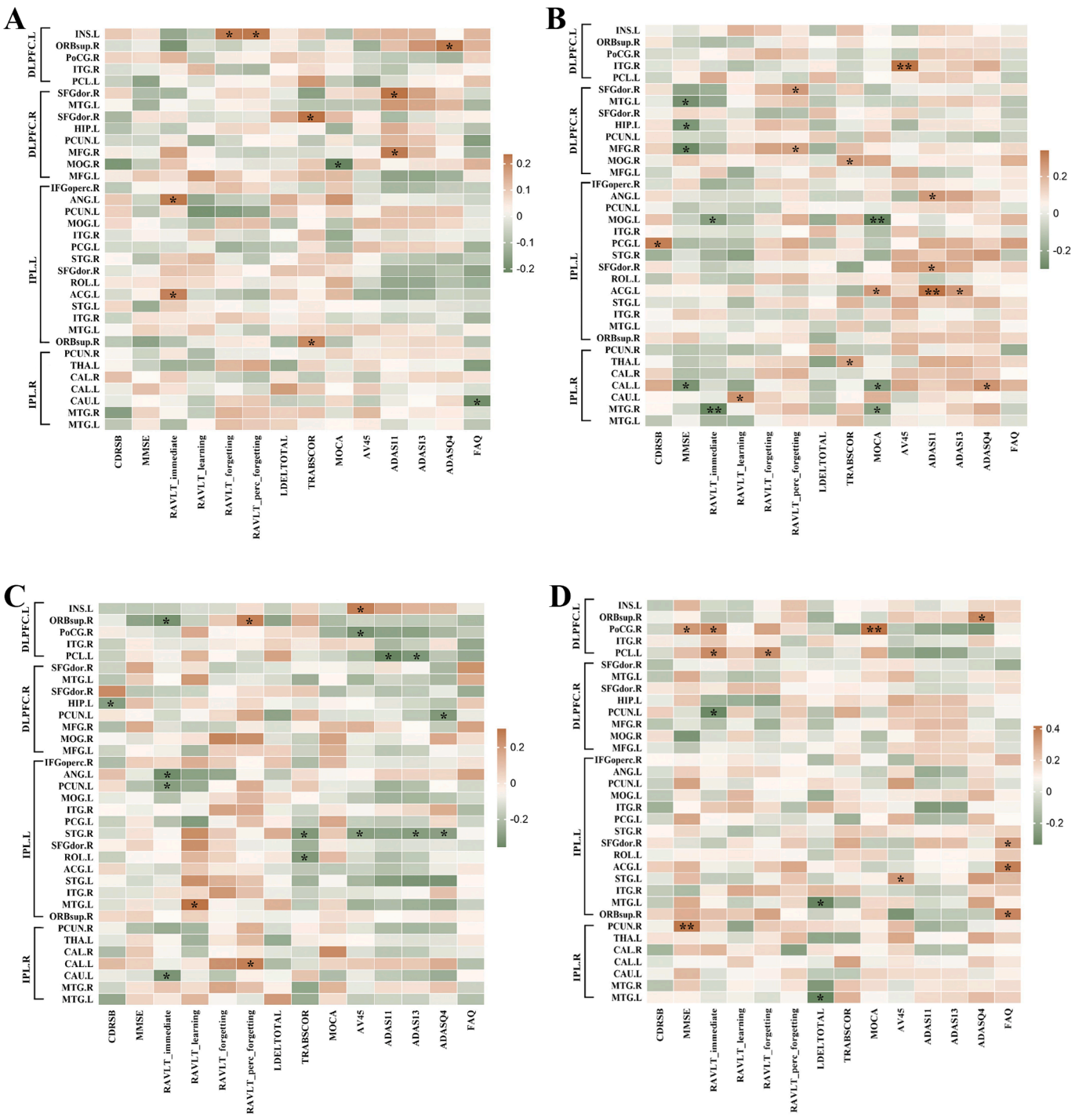

Fig. 5. Behavioural significance of ANOVA interactions and neuropsychological tests, including the CN (A), EMCI (B), LMCI (C), and AD groups (D). ACG, Anterior cingulate and paracingulate gyri; ANG, Angular gyrus; CAL, Calcarine fissure and surrounding cortex; CAU, Caudate nucleus; HIP, Hippocampus; IFG, Inferior frontal gyrus, opercular part; INS, Insula; ITG, Inferior temporal gyrus; MFG, Middle frontal gyrus; MOG, Middle occipital gyrus; MTG, Middle temporal gyrus; ORBmid, Middle frontal gyrus, orbital part; ORBsup, Superior frontal gyrus, orbital part; PCG, Posterior cingulate gyrus; PCL, Paracentral lobule; PCUN, Precuneus; PoCG, Postcentral gyrus; PreCG, Precentral gyrus; ROL, Rolandic operculum; SFGdor, Superior frontal gyrus, dorsolateral; STG, Superior temporal gyrus; THA, Thalamus. * Indicates a significant difference between groups, $p < 0.05$. ** Indicates a significant difference between groups, $p < 0.001$.

RAVLT_immediate ($r = 0.353$, $p = 0.02$) and forgetting ($r = 0.336$, $p = 0.027$).

4.4.2. *R-DLPFC network*

(1) Main effect of disease: According to results of the main effect of the disease, the FC from DLPFC.L to the frontal lobe (bilateral superior frontal gyrus, dorsolateral (SFGdor) and MFG.L) in CN individuals was significantly correlated with executive function and the ADAS11 score. Similarly, in the EMCI group, the FC between MTG.L ($r = -0.275$, $p = 0.016$), HIP.L ($r = -0.259$, $p = 0.023$), MFG.R ($r = -0.29$, $p = 0.011$) to DLPFC.R was significantly negatively correlated with MMSE score, while right superior frontal dorsolateral gyrus (SFGdor.R) ($r = 0.243$, $p = 0.033$) and MFG.R (($r = 0.225$, $p = 0.049$) were correlated with RAVLT_perc_forgetting score. In the LMCI group, FC in the HIP.L and

PCUN.R were significantly correlated with CDRSB ($r = -0.284$, $p = 0.042$) and ADASQ4 ($r = -0.301$, $p = 0.03$), respectively. (2) Main effect of gene: In the CN group, the FC of DLPFC.R to MOG.R was significantly negatively correlated with MoCA score ($r = -0.216$, $p = 0.028$). In the LMCI and AD groups, FC between brain regions with a gene main effect and the DLPFC.R was observed not significantly correlated with the clinical cognitive score. (3) Interaction of gene × disease: The brain regions influenced by interaction within the R-DLPFC network did not reach statistical significance.

4.4.3. L-IPL network

(1) Main effect of disease: In the CN group, the FC of ANG.L to IPL.L is correlated with the immediate score of situational memory ($r = 0.228$, $p = 0.02$). In the EMCI group, the FC of the ANG.L and left posterior cingulate gyrus were significantly positively correlated with cognitive scale scores (ADAS11 and CDRSB) ($r = 0.248$, $p = 0.03$; $r = 0.314$, $p = 0.005$), while the MOG.L was significantly negatively correlated with RAVLT_immediate ($r = -0.238$, $p = 0.037$) and MoCA ($r = -0.301$, $p = 0.008$). Similarly, in the LMCI group, the FC from ANG.L (($r = -0.338$, $p = 0.014$) and PCUN.L to IPL.L has negative correlation with RAVLT_immediate ($r = -0.283$, $p = 0.042$). (2) Main effect of gene: In the CN group, the FC between the left anterior cingulate and paracingulate gyri (ACG.L) was significantly positively correlated with RAVLT_Immediate ($r = 0.213$, $p = 0.003$), while in the ECMI group, it was significantly correlated with MoCA ($r = 0.242$, $p = 0.034$) and ADAS11/13 (($r = 0.343$, $p = 0.002$; $r = 0.243$, $p = 0.033$) scores. In addition, in the EMCI group, the FC between MOG.L ($r = -0.301$, $p = 0.008$) and SFGdor.L ($r = 0.238$, $p = 0.037$) was associated with cognitive scores of dementia (MoCA and ADAS11). In the LMCI group, the FC among the right STG in L-IPL network was significantly negatively correlated with multiple neurocognitive scale scores, including executive function ($r = -0.302$, $p = 0.029$), AV45 ($r = -0.285$, $p = 0.041$), ADAS13 ($r = -0.287$, $p = 0.039$), and ADASQ4 ($r = -0.279$, $p = 0.045$) scores. In the AD group, the FC in the SFGdor.R ($r = 0.304$, $p = 0.047$) and ACG.L ($r = 0.386$, $p = 0.011$)was significantly correlated with social function (FAQ). At the same time, the FC in STG was significantly correlated with AV45 ($r = 0.302$, $p = 0.049$). (3) Interaction of gene × disease: In the CN group, the FC from IPL.L to ORBsup.R has significantly correlation with the executive function scale (TRABSCORE) score ($r = 0.202$, $p = 0.004$). In the LMI group, there was a significantly correlation between the FC of IPL.L to MTG.L and RAVLT_learning ($r = 0.307$, $p = 0.027$). In the AD group, the FC in the MTG.L was significantly negatively correlated with LDELTOTAL ($r = -0.341$, $p = 0.025$). but was significantly positively correlated with the FC and FAQ in ORBsup.R ($r = 0.365$, $p = 0.016$).

4.4.4. R-IPL network

(1) Main effect of disease: Among the main effects of disease, only the FC between IPL.R and left thalamus in the EMCI group showed a significant correlation with executive function (TRABSCOR) ($r = 0.226$, $p = 0.048$). (2) Main effect of gene: In the CN group, there was a significant negative correlation between the FC in the right frontal gyrus and FAQ score ($r = -0.202$, $p = 0.04$). In the MCI group (including EMCI and LMCI), there were significant correlations between multiple cognitive scales such as MMSE, MoCA, RAVLT_learning and ADASQ4 and the FC from IPL.R to the left caudate nucleus and calcarine fissure and surrounding cortex. (3) Interaction of gene × disease: In the EMCI group, the FC from IPL.R to MTG.R was significantly negatively correlated with RAVLT_immediate ($r = -0.299$, $p = 0.008$) and MoCA scores ($r = -0.227$, $p = 0.047$). Similarly, in the AD group, the FC was significantly negatively correlated with LDELTOTAL score ($r = -0.34$, $p = 0.026$).

5. Discussion

This study focused on exploring whether carrying an AD risk gene could diminish effective functional connectivity of the ECN across AD-spectrum populations. We selected normal controls, EMCI, LMCI, and AD patients, both carriers and non-carriers of the APOE ε4 allele, to explore the longitudinal changes in ECN functional connectivity throughout the progression of AD.

5.1. Distinguishably variable patterns of impaired ECN in APOE ε4 carriers and non-carriers

5.1.1. Inverted U-shaped curve of fronto-parietal network

By comparison, APOE ε4 allele carriers exhibited greater functional connectivity in several regions, including the FC between parietal lobe and temporal lobe, the parietal lobe and the orbito-superior frontal gyrus, and the FC within frontal lobe, during normal cognitive functioning compared to non-carriers. Additionally, carriers showed stronger functional connectivity between the internal frontal lobe seed site (DLPFC. L-PCL) during the EMCI stage (Zhao et al., 2019; Ye et al., 2021; Fleisher et al., 2009). Previous research by Agosta (2012) found that MCI patients exhibited activation of the right ventral lateral and dorsolateral prefrontal brain regions relative to controls (Agosta et al., 2012; Grady et al., 2003). This discovery aligned with findings from other studies (Zhao et al., 2019; Sheline et al., 2010; Clément and Belleville, 2010). These findings all demonstrated that early disease carriers have stronger frontal lobe functional connectivity (Chen et al., 2020; Bai et al., 2009). The decline in metabolism in the frontal cortex of non-carriers is associated with normal aging. Intriguingly, compared to healthy controls, subjects with low MCI cognitive scores failed to show additional prefrontal activation and had reduced activation in posterior regions (Clément and Belleville, 2010). Similar results were demonstrated in our study; where FC within the prefrontal lobe was significantly weaker in carriers compared to non-carriers during both the LMCI and AD stages. In contrast, non-carriers showed stronger frontal lobe activity in both the LMCI and AD stages. Compared to controls, the FC within the frontal lobe exhibited a change curve with an inverted U-shaped curve of elevation followed by a decrease with cognitive decline. This pattern indicates that carriers experience a compensatory increase in frontal lobe connectivity in early stages to mitigate functional deficits, but this compensatory mechanism diminishes in later disease stages.

In this study, the carriers shows functional activation in the frontal lobe in the early stages of the disease and decreased activation in the later stages, and the opposite is true for the parietal lobe (Lustig et al., 2003; Zhao et al., 2018; Celone et al., 2006; Petrella et al., 2007). This may indicate that carriers rely primarily on the frontal lobes to maintain cognitive function in the early stages of the disease and that this dependence is lost in the later stages of the disease (Scarmeas and Stern, 2006). On the contrary, non-carriers showed stronger frontal activation in the late stage of the disease, so the difference between carriers and non-carriers in the frontal-parietal functional connectivity exhibits a change curve of decline followed by a rise followed by a fall, which looks like a combination of a positive and an inverted U-shaped curve (Zhao et al., 2018; Hafkemeijer et al., 2017). A study of resting-state functioning in AD patients showed that, compared to those in MCI patients and controls, opposite connectivity effects were associated with the DMN (reduced) and frontal network (enhanced) in the AD group (Agosta et al., 2012). In noncarriers, enhanced prefrontal connectivity within the ECN aims to sustain cognitive efficiency, an alteration that can be interpreted as a reliance on the prefrontal cortex to compensate for the reduced parietal activation in AD patients (Grady et al., 2003).

5.1.2. Positive U-shaped curve of parietal-temporal network

Carriers in the cognitively normal stage showed stronger rsFC between the parietal and temporal lobes, which may be explained by the fact that healthy carriers require more activation of brain regions to achieve and maintain performance levels similar to those of noncarriers (Clément and Belleville, 2010; Scarmeas et al., 2003). Preclinical enhancement of rsFC is beneficial to some extent. A study on asymptomatic Alzheimer's disease found that stronger connectivity in the executive control network during the preclinical stage of Alzheimer's

disease is associated with less cognitive decline (Boyle et al., 2024). Many studies have shown that healthy elderly individuals carrying the Apoe ε4 allele exhibit lower metabolism and more gray matter atrophy in the parietal lobe than non-carriers (Small et al., 1995; Nao et al., 2017; Goñi et al., 2013). However, our study observed stronger functional connectivity in the parietal-temporal lobe among carriers without early cognitive impairment. One possible explanation is that the atrophy of the medial temporal lobe occurs in the early stage of AD, which is more pronounced in carriers, leading to a significant decline in rsFC in the temporal lobe in early disease stages. In contrast, carriers show a trend of increased rsFC between the parietal and temporal lobes during the MCI and AD stages. A study by Jacobs (2012) showed that, compared to controls, patients with MCI and AD had increased activation in several temporal regions (middle and upper temporal gyrus, parahippocampal gyrus, (HIP)) and parietal regions (supramarginal gyrus, subparietal lobule, angular gyrus). Sorg (2007) reported enhanced rs-fMRI connectivity in the posterior cingulate gyrus and parietal cortex in patients with MCI, potentially compensating for reduced connectivity in the medial prefrontal cortex (Sorg et al., 2007). Increased neural activity in parietal and temporal regions represents a potential compensatory mechanism, wherein increased neural activity compensating for ineffective connectivity within the frontal lobe and between the frontal and parietal lobes (Agosta et al., 2012; Pihlajamäki et al., 2009; Jacobs et al., 2012). As disease progresses; functional connectivity in the parietal-temporal lobe showed the opposite change to that within the frontal lobe, with a positive U-shaped curve, as shown in Fig. 4A, B and C. This suggested that the functional impairment and compensatory patterns in carriers were different from those in non-carriers. Increased parietal activation reflects the involvement of dorsal pathways, which may be related to the function of the inferior parietal lobule. The subparietal lobule is involved in object recognition, spatial manipulation, and detection of salient stimuli and plays a role in sustained attention along with the prefrontal cortex.

5.2. Mechanisms of ECN compensation at different stages of disease associated with APOE ε4 allele

Our study showed that functional connectivity with regions associated with the inferior parietal lobe decreases followed by an increase with disease progression in individuals without APOE risk genes, whereas the reverse trend is observed in carriers (Bartrés-Faz et al., 2008). This seems to be consistent with the compensatory hypothesis that APOE ε4 carriers in early stages of the disease may require additional neurocognitive efforts, such as increased functional connectivity, activation of additional brain regions and increased blood flow, to maintain comparable levels of performance to non-carriers (Scarmeas et al., 2003). Several studies of healthy APOE ε4 carriers and non-carriers have shown that younger APOE ε4 carriers have better cognitive performance, a trend that reverses in APOE ε4 carriers in their 50 s (Mondadori et al., 2007; Han et al., 2007). During the AD phase, carriers exhibited weaker functional connectivity, which may be related to early compensatory depletion of their compensatory capacity. In conclusion, APOE4 carriers are more likely to have brain function hub regions resulting in Aβ deposition and accumulation, leading to carriers requiring more active functional activity to maintain cognitive function even when cognition is not impaired (Raulin et al., 2022; Lee et al., 2023). This also leads to poorer cognitive performance in carriers in the later stages of the disease.

6. Limitation

Our study found that functional connectivity within the ECN is influenced by APOE and disease state. The age-related decline in FC within the network is a sign of compromised specialized processing, a common phenomenon during aging (He et al., 2014). Our study participants were aged over 55 years, and the absence of younger controls leaves uncertainty regarding any age-related factors influencing our conclusions. To address this, future studies will include subjects aged 30–40 years who are carriers and non-carriers of the APOE gene. Additionally, several studies have shown that there is an interaction between female gender and the APOE gene. In our dataset, gender ratios did not differ significantly between groups, so gender was not used as a separate grouping criterion. We controlled for gender by including it as a covariate in ANOVA and correlation analyses to minimize its impact on results. However, this still cannot exclude the possibility that differences in the data are caused by females within groups. Since cerebrospinal fluid data collection is not mandatory, more than half of the participants lack cerebrospinal fluid data, making it impossible to conduct correlation analyses between functional connectivity, cerebrospinal fluid biomarkers, and cognitive performance. Future research will expand our sample size to address these limitations.

7. Conclusion

Current research suggests that ECN functional connectivity is influenced by the APOE ε4 allele and exhibits different impairment patterns between carriers and non-carriers. This heterogeneity in functional network changes among individuals with different genotypes in the early stages of disease is highly important for understanding potential biological markers implicated in Alzheimer's disease progression.

CRediT authorship contribution statement

Ruichen Han: Writing – original draft, Visualization, Software, Resources, Project administration, Methodology, Investigation, Formal analysis, Data curation, Conceptualization. **Xue Zhang:** Validation, Methodology, Formal analysis, Conceptualization. **Ya Chen:** Methodology, Investigation, Conceptualization. **Xinle Hou:** Software, Methodology, Investigation, Data curation, Conceptualization. **Feng Bai:** Writing – review & editing, Validation, Software, Methodology, Funding acquisition, Data curation.

Declaration of competing interest

The authors declare that they have no known competing financial interests or personal relationships that could have appeared to influence the work reported in this paper.

Data availability

Data will be made available on request.

Acknowledgements

This work was supported partly by grants from the National Natural Science Foundation of China (No. 82071186; 82371437), the Key Research and Development Program of Jiangsu Province (No. BE2023674), Clinical Trials from the Affiliated Drum Tower Hospital, Medical School of Nanjing University (No. 2022-LCYG-MS-05) and the Jiangsu Province Senior Health Project (No. LKZ2023014). The Alzheimer's Disease Neuroimaging Initiative (ADNI) was founded by Dr. Michael W. Weiner and received public and private funding from 20 companies, two foundations, and the National Institute on Aging. The data for this study were obtained from the ADNI database. The Alzheimer's Disease Treatment Institute (ATRI) at the University of Southern California participated in the research coordination work, and data dissemination was contributed by the Neuroimaging Laboratory at the University of Southern California. We would also want to express our gratitude to the researchers and volunteers at the ADNI site for their contributions to the research. The data processing, analysis, and interpretation of the results were all carried out by the member authors of this study.

Appendix. Supplementary data

Supplementary data to this article can be found online at https://doi.org/10.1016/j.brainres.2024.149229.

References

Agosta, F., Pievani, M., Geroldi, C., et al., 2012. Resting state fMRI in Alzheimer's disease: beyond the default mode network [J]. Neurobiol. Aging 33 (8), 1564–1578.

Bai, F., Watson, D.R., Yu, H., et al., 2009. Abnormal resting-state functional connectivity of posterior cingulate cortex in amnestic type mild cognitive impairment [J]. Brain Res. 1302, 167–174.

Bartrés-Faz, D., Serra-Grabulosa, J.M., Sun, F.T., et al., 2008. Functional connectivity of the hippocampus in elderly with mild memory dysfunction carrying the APOE epsilon4 allele [J]. Neurobiol. Aging 29 (11), 1644–1653.

Benson, G., Hildebrandt, A., Lange, C., et al., 2018. Functional connectivity in cognitive control networks mitigates the impact of white matter lesions in the elderly [J]. Alzheimers Res. Ther. 10 (1), 109.

Biswal, B., Yetkin, F.Z., Haughton, V.M., et al., 1995. Functional connectivity in the motor cortex of resting human brain using echo-planar MRI [J]. Magn. Reson. Med. 34 (4), 537–541.

Boyle, R., Klinger, H.M., Shirzadi, Z., et al., 2024. Left frontoparietal control network connectivity moderates the effect of amyloid on cognitive decline in preclinical Alzheimer's disease: the A4 study [J]. J. Prev Alzheimers Dis. 11 (4), 881–888.

Brown, J.A., Terashima, K.H., Burggren, A.C., et al., 2011. Brain network local interconnectivity loss in aging APOE-4 allele carriers [J]. PNAS 108 (51), 20760–20765.

Brugnolo, A., Morbelli, S., Arnaldi, D., et al., 2014. Metabolic correlates of Rey auditory verbal learning test in elderly subjects with memory complaints [J]. J. Alzheimers Dis. 39 (1), 103–113.

Cai, S., Peng, Y., Chong, T., et al., 2017. Differentiated effective connectivity patterns of the executive control network in progressive MCI: a potential biomarker for predicting AD [J]. Curr. Alzheimer Res. 14 (9), 937–950.

Caselli, R.J., Dueck, A.C., Osborne, D., et al., 2009. Longitudinal modeling of age-related memory decline and the APOE epsilon4 effect [J]. N. Engl. J. Med. 361 (3), 255–263.

Celone, K.A., Calhoun, V.D., Dickerson, B.C., et al., 2006. Alterations in memory networks in mild cognitive impairment and Alzheimer's disease: an independent component analysis [J]. J. Neurosci. 26 (40), 10222–10231.

Chen, H., Sheng, X., Luo, C., et al., 2020. The compensatory phenomenon of the functional connectome related to pathological biomarkers in individuals with subjective cognitive decline [J]. Transl. Neurodegener. 9 (1), 21.

Clément, F., Belleville, S., 2010. Compensation and disease severity on the memory-related activations in mild cognitive impairment [J]. Biol. Psychiatry 68 (10), 894–902.

Duan, X., Liao, W., Liang, D., et al., 2012. Large-scale brain networks in board game experts: insights from a domain-related task and task-free resting state [J]. PLoS One 7 (3), e32532.

Esposito, F., Goebel, R., 2011. Extracting functional networks with spatial independent component analysis: the role of dimensionality, reliability and aggregation scheme [J]. Curr. Opin. Neurol. 24 (4), 378–385.

Filippini, N., Macintosh, B.J., Hough, M.G., et al., 2009. Distinct patterns of brain activity in young carriers of the APOE-epsilon4 allele [J]. PNAS 106 (17), 7209–7214.

Fleisher, A.S., Sherzai, A., Taylor, C., et al., 2009. Resting-state BOLD networks versus task-associated functional MRI for distinguishing Alzheimer's disease risk groups [J]. Neuroimage 47 (4), 1678–1690.

Goñi, J., Cervantes, S., Arrondo, G., et al., 2013. Selective brain gray matter atrophy associated with APOE ε4 and MAPT H1 in subjects with mild cognitive impairment [J]. J. Alzheimers Dis. 33 (4), 1009–1019.

Grady, C.L., Bernstein, L.J., Beig, S., et al., 2002. The effects of encoding task on age-related differences in the functional neuroanatomy of face memory [J]. Psychol. Aging 17 (1).

Grady, C.L., Mcintosh, A.R., Beig, S., et al., 2003. Evidence from functional neuroimaging of a compensatory prefrontal network in Alzheimer's disease [J]. J. Neurosci. 23 (3), 986–993.

Hafkemeijer, A., Möller, C., Dopper, E.G.P., et al., 2017. A longitudinal study on resting state functional connectivity in behavioral variant frontotemporal dementia and Alzheimer's disease [J]. J. Alzheimers Dis. 55 (2), 521–537.

Han, S.D., Drake, A.I., Cessante, L.M., et al., 2007. Apolipoprotein E and traumatic brain injury in a military population: evidence of a neuropsychological compensatory mechanism? [J]. J. Neurol. Neurosurg. Psychiatry 78 (10), 1103–1108.

Hausman, H.K., Hardcastle, C., Albizu, A., et al., 2022. Cingulo-opercular and frontoparietal control network connectivity and executive functioning in older adults [J]. Geroscience 44 (2), 847–866.

He, X., Qin, W., Liu, Y., et al., 2014. Abnormal salience network in normal aging and in amnestic mild cognitive impairment and Alzheimer's disease [J]. Hum. Brain Mapp. 35 (7), 3446–3464.

Jacobs, H.I.L., Van Boxtel, M.P.J., Heinecke, A., et al., 2012. Functional integration of parietal lobe activity in early Alzheimer disease [J]. Neurology 78 (5), 352–360.

Koutsodendris, N., Nelson, M.R., Rao, A., et al., 2022. Apolipoprotein E and Alzheimer's disease: findings, hypotheses, and potential mechanisms [J]. Annu. Rev. Pathol. 17, 73–99.

Lee, S., Devanney, N.A., Golden, L.R., et al., 2023. APOE modulates microglial immunometabolism in response to age, amyloid pathology, and inflammatory challenge [J]. Cell Rep. 42 (3), 112196.

Lustig, C., Snyder, A.Z., Bhakta, M., et al., 2003. Functional deactivations: change with age and dementia of the Alzheimer type [J]. PNAS 100 (24), 14504–14509.

Mcdade, E., Llibre-Guerra, J.J., Holtzman, D.M., et al., 2021. The informed road map to prevention of Alzheimer Disease: a call to arms [J]. Mol. Neurodegener. 16 (1), 49.

Mcguinness, B., Barrett, S.L., Craig, D., et al., 2010. Executive functioning in Alzheimer's disease and vascular dementia [J]. Int. J. Geriatr. Psychiatry 25 (6), 562–568.

Mishra, S., Blazey, T.M., Holtzman, D.M., et al., 2018. Longitudinal brain imaging in preclinical Alzheimer disease: impact of APOE ε4 genotype [J]. Brain 141 (6), 1828–1839.

Miyake, A., Friedman, N.P., Emerson, M.J., et al., 2000. The unity and diversity of executive functions and their contributions to complex "Frontal Lobe" tasks: a latent variable analysis [J]. Cogn. Psychol. 41 (1).

Mondadori, C.R.A., De Quervain, D.J.F., Buchmann, A., et al., 2007. Better memory and neural efficiency in young apolipoprotein E epsilon4 carriers [J]. Cereb. Cortex 17 (8), 1934–1947.

Nao, J., Sun, H., Wang, Q., et al., 2017. Adverse effects of the apolipoprotein E ε4 allele on episodic memory, task switching and gray matter volume in healthy young adults [J]. Front. Hum. Neurosci. 11, 346.

Pardo, J.V., Lee, J.T., Sheikh, S.A., et al., 2007. Where the brain grows old: decline in anterior cingulate and medial prefrontal function with normal aging [J]. Neuroimage 35 (3), 1231–1237.

Petrella, J.R., Prince, S.E., Wang, L., et al., 2007. Prognostic value of posteromedial cortex deactivation in mild cognitive impairment [J]. PLoS One 2 (10), e1104.

Pihlajamäki, M., Jauhiainen, A.M., Soininen, H., 2009. Structural and functional MRI in mild cognitive impairment [J]. Curr. Alzheimer Res. 6 (2), 179–185.

Raulin, A.-C., Doss, S.V., Trottier, Z.A., et al., 2022. ApoE in Alzheimer's disease: pathophysiology and therapeutic strategies [J]. Mol. Neurodegener. 17 (1), 72.

Scarmeas, N., Stern, Y., 2006. Imaging studies and APOE genotype in persons at risk for Alzheimer's disease [J]. Curr. Psychiatry Rep. 8 (1), 11–17.

Scarmeas, N., Zarahn, E., Anderson, K.E., et al., 2003. Cognitive reserve modulates functional brain responses during memory tasks: a PET study in healthy young and elderly subjects [J]. Neuroimage 19 (3), 1215–1227.

Scheltens, P., De Strooper, B., Kivipelto, M., et al., 2021. Alzheimer's disease [J]. Lancet 397 (10284), 1577–1590.

Sheline, Y.I., Morris, J.C., Snyder, A.Z., et al., 2010. APOE4 allele disrupts resting state fMRI connectivity in the absence of amyloid plaques or decreased CSF Aβ42 [J]. J. Neurosci. 30 (50), 17035–17040.

Small, G.W., Mazziotta, J.C., Collins, M.T., et al., 1995. Apolipoprotein E type 4 allele and cerebral glucose metabolism in relatives at risk for familial Alzheimer disease [J]. J. Am. Med. Assoc. 273 (12), 942–947.

Song, X., Panych, L.P., Chen, N.-K., 2016. Data-driven and predefined ROI-based quantification of long-term resting-state fMRI reproducibility [J]. Brain Connect. 6 (2), 136–151.

Sorg, C., Riedl, V., Mühlau, M., et al., 2007. Selective changes of resting-state networks in individuals at risk for Alzheimer's disease [J]. PNAS 104 (47), 18760–18765.

Vincent, J.L., Kahn, I., Snyder, A.Z., et al., 2008. Evidence for a frontoparietal control system revealed by intrinsic functional connectivity [J]. J. Neurophysiol. 100 (6), 3328–3342.

Wang, J., Wang, X., He, Y., et al., 2015. Apolipoprotein E ε4 modulates functional brain connectome in Alzheimer's disease [J]. Hum. Brain Mapp. 36 (5), 1828–1846.

Wang, Z., Yan, C., Zhao, C., et al., 2011. Spatial patterns of intrinsic brain activity in mild cognitive impairment and Alzheimer's disease: a resting-state functional MRI study [J]. Hum. Brain Mapp. 32 (10), 1720–1740.

Wee, C.-Y., Yap, P.-T., Zhang, D., et al., 2014. Group-constrained sparse fMRI connectivity modeling for mild cognitive impairment identification [J]. Brain Struct. Funct. 219 (2), 641–656.

Ye, Q., Chen, H., Liu, R., et al., 2021. Lateralized contributions of medial prefrontal cortex network to episodic memory deficits in subjects with amnestic mild cognitive impairment [J]. Front. Aging Neurosci. 13, 756241.

Yeo, B.T.T., Krienen, F.M., Sepulcre, J., et al., 2011. The organization of the human cerebral cortex estimated by intrinsic functional connectivity [J]. J. Neurophysiol. 106 (3), 1125–1165.

Zhao, Q., Lu, H., Metmer, H., et al., 2018. Evaluating functional connectivity of executive control network and frontoparietal network in Alzheimer's disease [J]. Brain Res. 1678, 262–272.

Zhao, Q., Sang, X., Metmer, H., et al., 2019. Functional segregation of executive control network and frontoparietal network in Alzheimer's disease [J]. Cortex 120, 36–48.